Pharmaceutical Research, Vol. 24, No. 2, February 2007 (© 2006)
DOI: 10.1007/s11095-006-9173-4

Featured Article

Spatio–temporal VEGF and PDGF Delivery Patterns Blood Vessel Formation and Maturation

Ruth R. Chen,[1,2] Eduardo A. Silva,[2] William W. Yuen,[2] and David J. Mooney[2,3]

Received July 20, 2006; accepted October 3, 2006; published online December 27, 2006

Purpose. Biological mechanisms of tissue regeneration are often complex, involving the tightly coordinated spatial and temporal presentation of multiple factors. We investigated whether spatially compartmentalized and sequential delivery of factors can be used to pattern new blood vessel formation.
Materials and Methods. A porous bi-layered poly(lactide–co-glycolide) (PLG) scaffold system was used to locally present vascular endothelial growth factor (VEGF) alone in one spatial region, and sequentially deliver VEGF and platelet-derived growth factor (PDGF) in an adjacent region. Scaffolds were implanted in severely ischemic hindlimbs of SCID mice for 2 and 6 weeks, and new vessel formation was quantified within the scaffolds.
Results. In the compartment delivering a high dose of VEGF alone, a high density of small, immature blood vessels was observed at 2 weeks. Sequential delivery of VEGF and PDGF led to a slightly lower blood vessel density, but vessel size and maturity were significantly enhanced. Results were similar at 6 weeks, with continued remodeling of vessels in the VEGF and PDGF layer towards increased size and maturation.
Conclusions. Spatially localizing and temporally controlling growth factor presentation for angiogenesis can create spatially organized tissues.

KEY WORDS: angiogenesis; vascular remodeling; controlled drug delivery; VEGF; PDGF.

INTRODUCTION

The development of organized tissues and organs (i.e. blood vessels, nerves, bone) (1–3) often results from the spatially and temporally organized signaling of multiple growth factors. Angiogenesis is one such mechanism controlled by a complex cascade of events. The formation of mature new vascular networks requires initiation by a pro-angiogenic growth factor such as vascular endothelial growth factor (VEGF), and subsequent vessel stabilization by platelet-derived growth factor (PDGF) mediated smooth muscle cell (SMC) and pericyte recruitment (4,5). VEGF and its isoforms (6), and other angiogenic growth factors act in spatio–temporal gradients to regulate vessel density, size, and distribution to pattern vascular networks (7). Spatial control over angiogenesis is particularly important since undirected vessel growth can lead to pathological effects, and incorrect vascular patterning can lead to vessel instability and poor network functionality (7).

The biological mechanisms of angiogenesis imply that strategies to create new blood vessels may benefit from controlled spatio–temporal delivery of multiple factors to guide tissue regeneration (8,9). Current approaches to therapeutic angiogenesis for ischemic diseases (e.g. coronary artery disease, peripheral vascular disease) focus on the delivery of single growth factors in a bolus injection, and the lack of control over growth factor availability using this approach may be a factor in its limited clinical success to date (8,9). Researchers have addressed the need for spatio–temporal growth factor delivery by immobilizing single growth factors on substrates (10,11) or by arranging individual delivery vehicles (12). However, with these approaches, the sustained release of bioactive growth factors *in vivo* remains a challenge. Therefore, we have adapted a polymeric poly (lactide–co-glycolide) (PLG) scaffold system to allow localized and sustained delivery of multiple factors in discrete spatial distributions and used this system to determine if one can spatially control the formation of tissues.

Controlled delivery of VEGF using a PLG scaffold system has been previously demonstrated to overcome the challenges of sustained factor bioactivity and localized delivery associated with bolus injection delivery methods (13). Localized and sustained delivery of VEGF through a PLG scaffold system has also been shown to increase vessel density, and lead to the formation of functional vasculature (14), and this PLG delivery system has been adapted to allow sequential delivery of VEGF and PDGF, resulting in the

[1] Department of Biomedical Engineering, University of Michigan, Ann Arbor, Michigan, USA.
[2] Division of Engineering and Applied Sciences, Harvard University, Cambridge, Massachusetts, USA.
[3] To whom correspondence should be addressed. (e-mail: mooneyd@deas.harvard.edu)

formation of larger, more mature vessels (15). An additional benefit of this model is that the scaffold itself represents an area of *de novo* tissue formation, allowing one to examine the effects of growth factor induced angiogenesis alone, without the additional effects of arteriogensis of existing vessels in the surrounding tissue.

In this report, we investigate whether a controlled delivery system capable of spatially restricting growth factor delivery to layers within a single scaffold can spatio–temporally control VEGF and PDGF delivery, and exert control over vascular patterning (i.e. vessel density, size, maturity) in an ischemic site. The ability to locally deliver multiple, spatially segregated factors in one vehicle over extended periods of time *in vivo* may enable the recreation of biologically relevant regeneration niches. In addition to serving as therapeutic tools, delivery systems capable of controlled spatio–temporal growth factor delivery may serve as valuable model systems to study the actions of multiple growth factors in other biological processes.

MATERIALS AND METHODS

Scaffold Fabrication

Scaffolds were fabricated from mixtures of poly(lactide–co-glycolide) (PLG) (85:15, intrinsic viscosity = 0.8 dl/g; and 75:25, intrinsic viscosity = 0.26 dl/g) (Alkermes, Cambridge, MA) microspheres (diameter = 5-100 μm) formed by standard double emulsion (16). In scaffolds containing PDGF, 75:25 PLG microspheres pre-encapsulated with PDGF at a loading concentration of 2 μg PDGF/mg PLG were used. Mixtures of PLG microspheres were lyophilized with or without $VEGF_{165}$ (Biological Resources Branch of the National Cancer Institute, Bethesda, MD) in a solution of MVM alginate (5% of total polymer mass) (ProNova, Oslo, Norway) as previously described (15). Each layer of the scaffold was mixed separately, and manually compacted in the scaffold die. Layers were compacted on top of each other and then finally compressed at 1,500 psi in a Carver press for 1 min to form a single scaffold. Each scaffold layer was formed from 3 mg of PLG total and 50 mg of salt (250 μm < d < 425 μm) with dimensions of 4.7 mm in diameter and 1.5 mm in thickness. Pressed scaffolds were processed using the gas-foaming/particulate-leaching method as previously described (13,17) to form structurally continuous vehicles. Total protein loaded following fabrication was 1.5 μg of VEGF and/or 3 μg PDGF in scaffold layer 1, and 3 μg VEGF alone in scaffold layer 2. Four conditions were examined with different combinations of growth factors in layer 1/layer 2: blank/blank (B/B), PDGF/blank (P/B), VEGF/VEGF (V/V), and VEGF-PDGF/VEGF (VP/V).

Analysis of Growth Factor Distribution within Layered Scaffolds

Scaffolds were fabricated as described above, but using Alexa Fluor 488 conjugated BSA (Molecular Probes, Carlsbad, CA) in place of VEGF to examine the spatial distribution of incorporated protein. Scaffolds embedded in growth factor reduced Matrigel (BD Biosciences, Franklin Lakes, NJ) were imaged using a Leica MZFL III stereo-dissecting fluorescence microscope (Leica Microsystems, Bannockburn, IL).

Mathematical Modeling

The mathematical model describes the VEGF profile as a result of diffusion, release from the scaffold, and degradation (18,19). The governing equation of the VEGF concentration, c, in each of the two layers of the scaffold is:

$$\frac{\partial c_i}{\partial t} = D_V \nabla^2 c_i + k_r c_{oi} - k_c c_i; \quad i = 1,2$$

where the index i refers to the layer. The diffusion coefficient of VEGF, $D_V = 7.0 \times 10^{-7}$ cm^2/s, was determined experimentally by quantifying diffusion of fluorescently labeled VEGF in Matrigel (BD Biosciences, Franklin Lakes, NJ). The fluorescence intensity of VEGF across the Matrigel was monitored over time to calculate the diffusion coefficient using the mean-square displacement equation for diffusion (20). The VEGF generation term is the product of the release rate, k_r, and the initial concentration within the polymer layer of the scaffold at implantation, c_{oi}. The release of VEGF is approximated to have two linear regions: a quick release in the first 2 days and a slower release subsequently. From profiles of VEGF release from this scaffold system (next section), the release rate k_r was determined to be 2.3×10^{-6} s^{-1} during the first 2 days and 4.7×10^{-7} s^{-1} subsequently. The VEGF degradation rate of 2.31×10^{-4} s^{-1} was determined experimentally from an *in vitro* assay. Briefly, VEGF was incubated with human dermal microvascular endothelial cells (HDMECs; Cambrex, East Rutherford, NJ) from 0-480 min. Conditioned media was collected, concentrated, diluted in fresh media, and added to new plates of HDMECs. Cell proliferation was quantified and normalized to control conditions containing fully bioactive VEGF to determine VEGF bioactivity over time using methods similar to those previously described (21). The steady-state system was solved in COMSOL Multiphysics using the 2D axial symmetric diffusion analysis tool with direct UMFPACK method.

Quantification of Growth Factor Release Kinetics

The kinetics of VEGF release from each layer of the scaffold were determined using ^{125}I-labeled recombinant human VEGF (Perkin Elmer, Boston, MA) as a tracer. Scaffolds were fabricated as described with the addition of 0.11 μCi radiolabeled VEGF mixed with the bulk quantity of unlabeled VEGF. The total radioactivity of each scaffold layer ($n = 4$) was counted in a gamma counter prior to incubation at 37°C in 4 ml of PBS containing Ca^{2+} and Mg^{2+}. At specific time points, 1 ml of the release solution was removed and the scaffold was placed in fresh release solution. The radioactivity of the release solution was measured using a WIZARD Automatic Gamma Counter (Perkin Elmer). The cumulative VEGF released from the scaffold at each time point was calculated as a percentage of total protein incorporated. PDGF release profiles were determined in the same manner using ^{125}I-PDGF (Perkin Elmer) as the tracer.

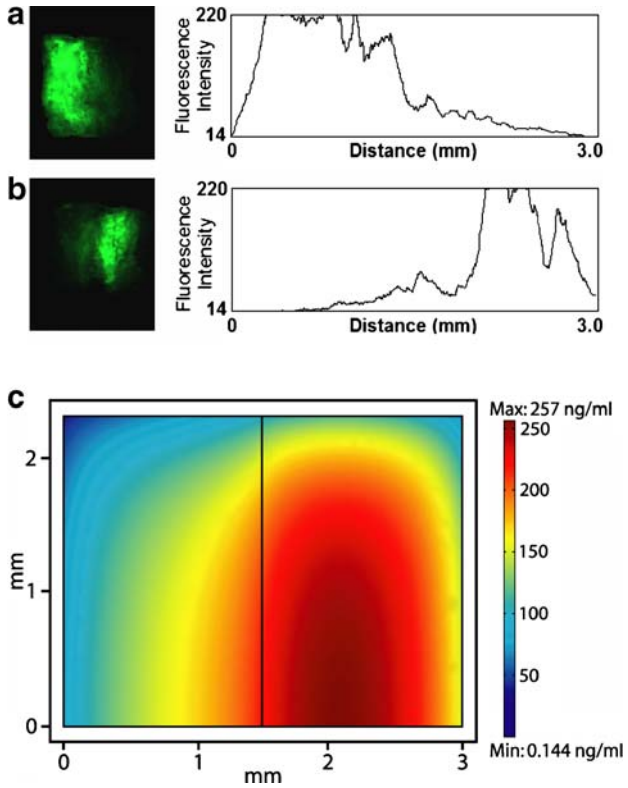

Fig. 1. Protein incorporated in each layer of the scaffold remained distinctly confined in that layer. Scaffolds were fabricated containing fluorescently labeled protein in layer 1 (a), or layer 2 (b), and imaged to examine the protein distribution in each layer following fabrication. The plots of fluorescence intensity over the entire length of the scaffold show sharp segregation of protein between layers. Mathematical modeling also predicts that a gradient in protein concentration during its release from the scaffold will persist in the tissue filling the pores of the scaffold at steady-state (c). A concentration profile of VEGF in layer 1 and layer 2 at steady-state is shown in a 2-D cross-section through the scaffold with axial symmetry through the zero *y*-axis.

Mouse Model of Hindlimb Ischemia and Scaffold Implantation

Layered scaffolds were implanted in 7-8 week-old SCID mice (Taconic, Hudson, NY) that had undergone unilateral ligation of hindlimb blood vessels to create a severe model of hindlimb ischemia (14). Briefly, animals were anesthetized by IP injection of a ketamine and xylazine cocktail. The entire hindlimb was shaved and sterilized prior to making an incision through the dermis. The external iliac artery and vein, and the femoral artery and vein were ligated using 5-0 Ethilon (Ethicon, Somerville, NJ). The vessels were severed between the ligation points, and a layered polymer scaffold was implanted with an orientation such that layer 1 was directly over the sites of ligation and layer 2 extended into the muscles of the inner thigh. At 2 and 6 weeks post-surgery, implanted polymer scaffolds were collected for histological analysis.

Immunohistochemistry and Blood Vessel Quantification

Scaffolds ($n = 5$/timepoint/experimental condition) were retrieved after 2 and 6 weeks, fixed in Z-fix (Anatech, Battle Creek, MI) overnight and changed into 70% EtOH for storage prior to histologic processing. Samples were embedded in paraffin and sectioned onto slides. Sections were immunostained with a monoclonal antibody raised against mouse CD31 (diluted 1:250) (Pharmingen, San Diego, CA) using the Tyramide Signal Amplification (TSA) Biotin System (Perkin Elmer Life Sciences, Boston, MA) to enhance detection. Briefly, deparaffinized sections were rehydrated, blocked for endogenous peroxidase activity and non-specific interactions, and incubated overnight at 4°C with the primary CD31 antibody. Sections were then incubated with an anti-rat mouse absorbed biotinylated secondary (diluted 1:200) (Vector Laboratories, Burlingame, CA). A tertiary TSA strepavidin antibody was applied, followed by a TSA biotinyl tyramide amplification solution for 7 min. The tertiary antibody was then reapplied. Staining was developed using DAB+ substrate chromogen (DAKO, Carpinteria, CA). Sections were counterstained with hematoxylin.

Immunostaining for α-smooth muscle actin (α-SMA) was performed by the Histology Core Facility at the Beth

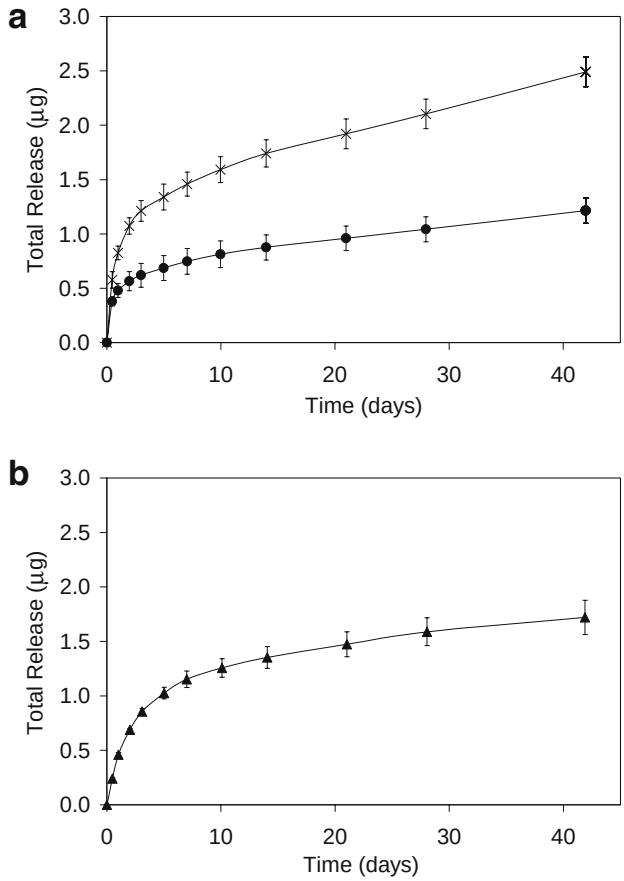

Fig. 2. VEGF (a) and PDGF (b) release from layered scaffolds was determined using radiolabeled growth factor ($n = 4$). The overall release profile of VEGF (a) is similar in layer 1 (-✕-) and layer 2 (-●-) with an initial burst of VEGF followed by a steady release. Pre-encapsulation of PDGF in PLG microspheres slowed its release from layer 1 of scaffolds (b, -▲-). The quantity of VEGF and PDGF released was proportional to the total mass of growth factor incorporated in each layer (1.5 μg VEGF and/or 3 μg PDGF in layer 1; 3 μg VEGF in layer 2). Values represent mean and standard deviation.

Israel Deaconess Medical Center. Briefly, deparaffinized and rehydrated sections were blocked for endogenous peroxidase activity and non-specific binding. Sections were incubated with an alkaline phosphatase-conjugated antibody to smooth muscle actin (Sigma) (1:50) for 2 h at room temperature. Staining was detected through incubation with Vector Red substrate solution (Vector Laboratories) for 20 min. Sections were counterstained with hematoxylin.

Sections from each sample were visualized at 100× and 200× with a Nikon light microscope (Indianapolis, IN) connected to a SPOT digital image capture system (Diagnostic Instruments, Sterling Heights, MI). Images were taken of entire scaffold sections at 100× and merged into a complete image of the section using Photoshop Elements (Adobe Systems, San Jose, CA). Vessel density and α-SMA positive vessel density were manually determined in the entire scaffold area as previously described (13,14). Vessel size was determined using IPLab 3.7 software (Scanalytics, Rockville, MD), again as previously described (13).

RESULTS AND DISCUSSION

Many therapeutic approaches to replace diseased or damaged tissues (e.g. bone, nerves, blood vessels) depend on complex tissue regeneration processes directed by the spatial and temporal presentation of growth factors. These studies describe a system capable of controlled spatial and temporal presentation of multiple growth factors, and the ability of this system to direct the organization of newly formed tissue was demonstrated in the context of angiogenesis. Control over vascular patterning using VEGF and PDGF may have broad implications in therapies to treat ischemic diseases.

Growth Factor Incorporation and Release from Layered Scaffolds

The protein incorporated into each layer of the scaffold remained confined to that layer after the gas foaming and particulate leaching method was used to form structurally

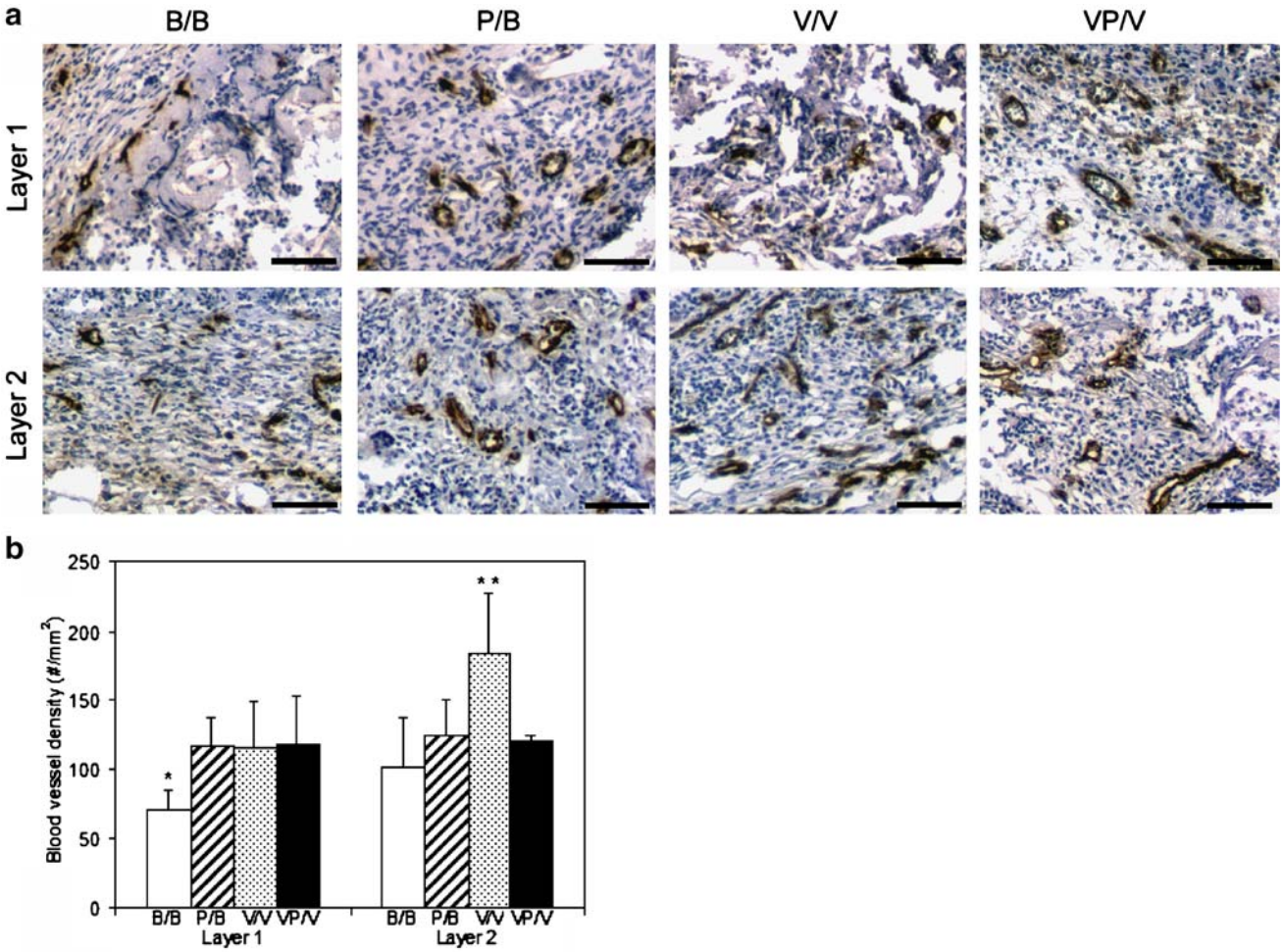

Fig. 3. Blood vessel densities within layered scaffolds 2 weeks post-implantation ($n = 5$). Representative images of CD31 stained sections of layer 1 and layer 2 (a) of scaffolds implanted in ischemic hindlimbs. Blood vessel density is increased in PDGF/blank (P/B), VEGF/VEGF (V/V), and VEGF-PDGF/VEGF (VP/V) scaffolds compared to blank/blank (B/B) scaffolds at 2 weeks. Scale bar equals 100 μm. Quantification of vessel densities (b) within each layer of implanted scaffolds revealed that VEGF and/or PDGF delivery in layer 1 resulted in vessel density elevated above control at 2 weeks. In layer 2, delivery of VEGF alone resulted in increased vascularity above all other conditions. Layer 1/layer 2: blank/blank (B/B), PDGF/blank (P/B), VEGF/VEGF (V/V), VEGF-PDGF/VEGF (VP/V). *, **$p < 0.05$ for vessel density in that layer compared to all other conditions in the same layer. Values represent mean and standard deviation.

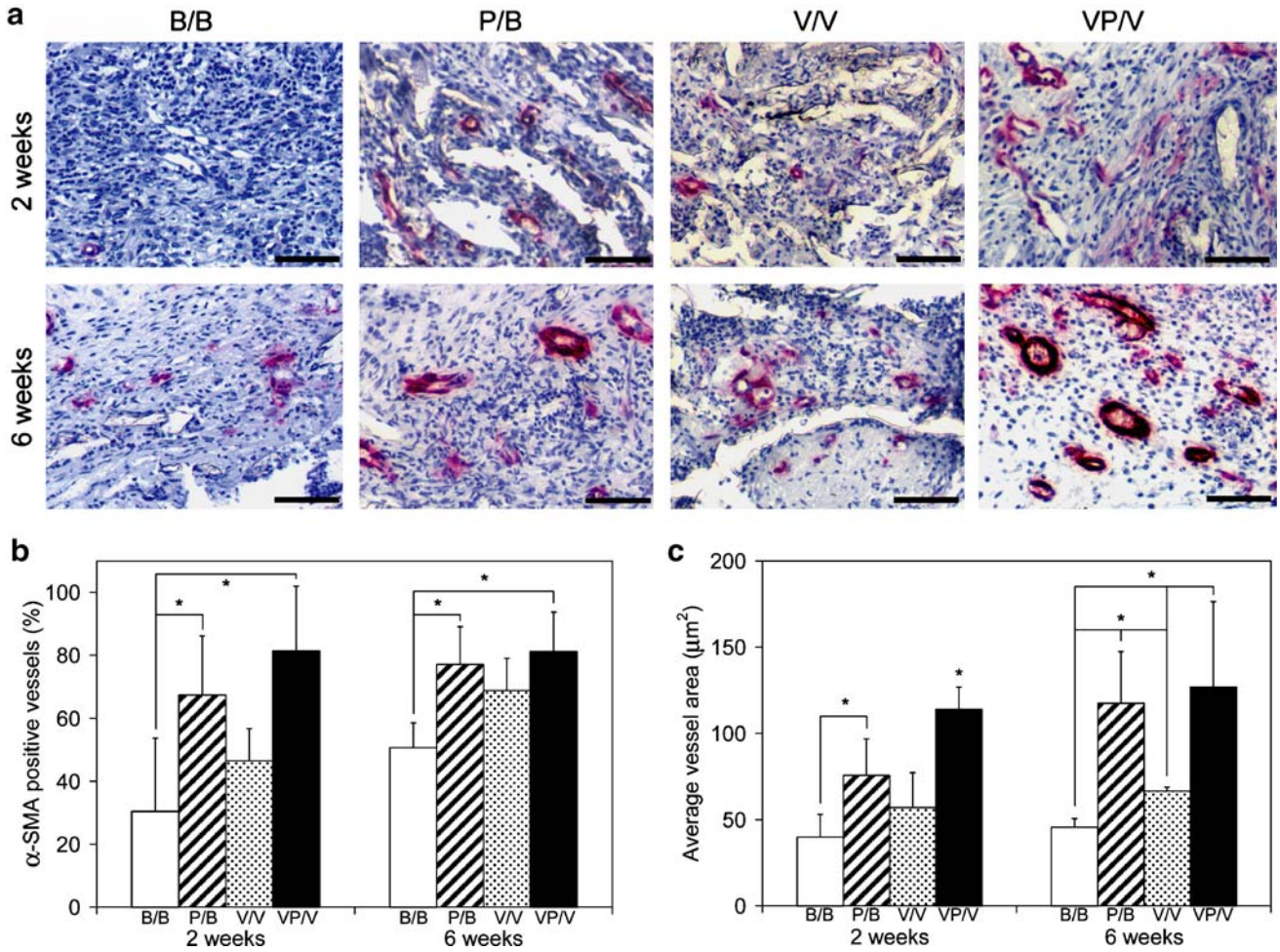

Fig. 4. Scaffolds sections were stained for α-SMA to examine vessel maturity in layer 1 (a) of scaffolds implanted in ischemic hindlimbs ($n = 5$). The percentage of α-SMA positive blood vessels (i.e. SMC stabilized vessels) at 2 and 6 weeks in layer 1 (b) was higher with PDGF delivery compared to control. The cross-sectional area of blood vessels in layer 1 (c) was also larger in conditions with PDGF delivery at both time points. Layer 1/layer 2: blank/blank (B/B), PDGF/blank (P/B), VEGF/VEGF (V/V), VEGF-PDGF/VEGF (VP/V). Scale bar equals 100 μm. $^*p < 0.05$. Values represent mean and standard deviation.

continuous delivery vehicles (Fig. 1a,b). During release, the bulk of the protein remained within the area of the scaffold where the protein was incorporated, and modeling of growth factor distribution within the scaffold indicated that a spatial distribution defined by the design of the scaffold may be maintained over time (Fig. 1c). The profile of VEGF release from the bulk of each layer of the scaffold was similar, with a quick burst followed by a sustained release (Fig. 2a). Therefore, the quantity of VEGF released from each layer varied based on the initial total mass of VEGF loaded. In addition to VEGF, PDGF was incorporated in the scaffold system to provide a signal for vessel maturation. The release of PDGF was delayed, in relation to VEGF, by pre-encapsulation of PDGF in the 75:25 PLG microspheres that were fused together in the foaming process to form the PLG scaffolds. PDGF was released in a slow sustained manner (Fig. 2b), and the quantity of PDGF released was relative to the total PDGF initially loaded in microspheres within the layer. This layered scaffold system allowed compartmentalization of incorporated growth factor and formed spatially distinct regions of release.

Density of Neovasculature within Layered Scaffolds

Scaffolds were subsequently implanted into the ischemic hindlimbs of SCID mice to examine their utility in patterning the new vasculature that forms within the volume of tissue defined by the scaffold. The SCID mouse model allows one to more readily distinguish changes in vasculature due to growth factor delivery because they display a more severe ischemic response compared to normal mice and do not recover naturally from ischemic injury (22–24). Total protein loading following fabrication was 1.5 μg of VEGF and/or 3 μg PDGF in scaffold layer 1, and 3 μg VEGF alone in scaffold layer 2. Four conditions were examined with different combinations of growth factors in layer 1/layer 2: blank/blank (B/B), PDGF/blank (P/B), VEGF/VEGF (V/V), and VEGF-PDGF/VEGF (VP/V).

The blood vessel density (BVD) within scaffold tissue was quantified from scaffold sections stained for the endothelial marker CD31 (Fig. 3a). In scaffolds retrieved at week 2, delivery of either VEGF or PDGF in P/B, V/V, and VP/V conditions resulted in a two-fold increase in BVD over blank

scaffolds in layer 1 (Fig. 3b). Delivery of VEGF in layer 2 of V/V scaffolds resulted in a nearly two-fold increase in BVD over all other conditions, with a higher BVD in layer 2 than layer 1 at 2 weeks (Fig. 3b). This result is consistent with expectations based on the lower VEGF dose delivered in layer 1, as compared to the higher VEGF dose delivered in layer 2. However, a similar increase in BVD was not observed with VEGF delivery in layer 2 of the VP/V condition at 2 weeks (Fig. 3b), possibly due to premature stabilization of neovessels by the presence of PDGF.

Maturation of Neovasculature within Layered Scaffolds

Neovascular remodeling contributes greatly to overall network maturation and stability (7), and the percentage of vessels stabilized with associated α-SMA positive SMCs and vessel cross-sectional areas were quantified in layer 1 (Fig. 4) and layer 2 (Fig. 5) of tissue within scaffolds at 2 and 6 weeks. In general, PDGF delivery produced larger, more mature vessels as the compartments delivering PDGF not only had higher percentages of SMC-invested vessels, but also had larger average vessel cross-sectional areas (Figs. 4 and 5). The differences in neovascular maturity due to PDGF delivery were most pronounced in layer 1, as anticipated.

The percentage of α-SMA positive vessels increased two-fold with PDGF delivery in P/B and VP/V conditions over control in both layers 1 and 2 at 2 weeks (Figs. 4 and 5). In layer 1, the percentage of α-SMA positive vessels increased ~20% in B/B and V/V conditions from 2 to 6 weeks, while the proportion of SMC invested vessels remained unchanged in P/B and VP/V conditions (Fig. 4B). In layer 2, the percentage of α-SMC positive vessels was elevated, but not statistically higher, in P/B and VP/V conditions over B/B and V/V scaffolds at both timepoints (Fig. 5b). Most vessels induced by the delivery of VEGF alone in layer 2 were in an immature state, with less than 50% of vessels being α-SMA positive at 2 weeks (Fig. 5), supporting the importance of a maturation signal such as PDGF in enhancing vessel maturity and size (25). Additionally, in layer 2 of all conditions, the percentage of α-SMA positive vessels increased ~20% from week 2 to week 6 (Fig. 5b). Vessel cross-sectional areas were two-fold larger in conditions with PDGF delivery than in B/B or V/V conditions in both layer 1 (Fig. 4c) and layer 2 at both time points (Fig. 5c). Vessels within V/V scaffolds were

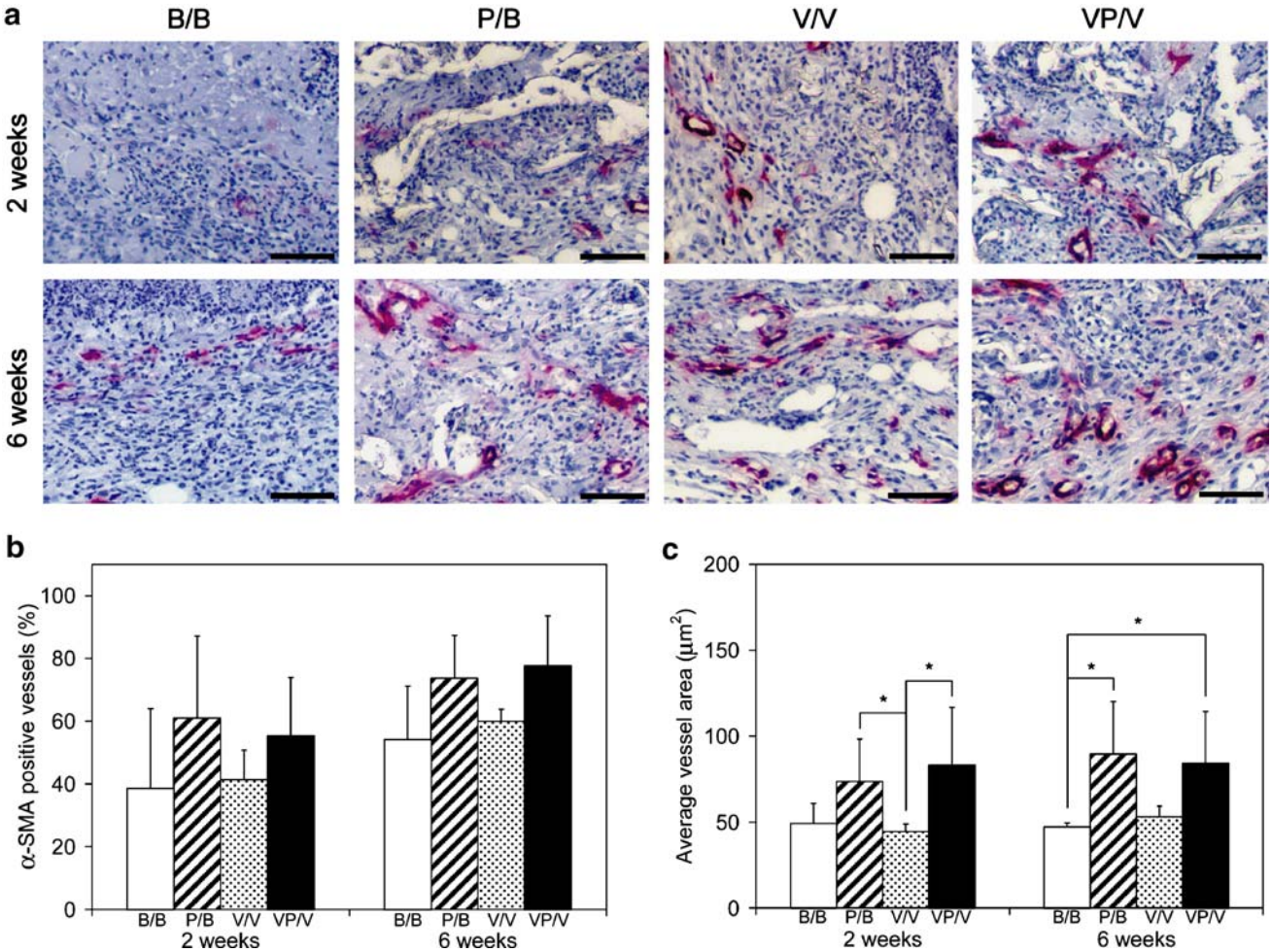

Fig. 5. Representative images of sections stained for **α**-SMA from layer 2 (a) of scaffolds implanted in ischemic hindlimbs at 2 and 6 weeks. In layer 2, PDGF delivering conditions showed elevated, but not significantly increased SMC association with vessels at both time points (b). However, PDGF delivery led to blood vessels with larger cross-sectional areas at 2 and 6 weeks post-implantation. Layer 1/layer 2: blank/blank (B/B), PDGF/blank (P/B), VEGF/VEGF (V/V), VEGF-PDGF/VEGF (VP/V). Scale bar equals 100 μm. $*p < 0.05$. Values represent mean and standard deviation.

smaller than vessels in PDGF delivering conditions, and at both 2 and 6 weeks the delivery of a higher dose of VEGF in layer 2 led to the formation of smaller vessels in layer 2 (Fig. 5c) as compared to layer 1 (Fig. 4c). Overall, the size of new vessels was affected by the spatial delivery of VEGF, but depended primarily on the presence of PDGF (Figs. 4c and 5c). These results taken together indicate that vessel maturation increased over time, and was enhanced by the delivery of PDGF in layer 1.

In summary, a controlled growth factor delivery system was developed for controlled release of VEGF and PDGF from spatially defined compartments. Protein incorporated in these layered scaffolds remained spatially restricted after completion of the fabrication process, allowing the spatially segregated delivery of VEGF and PDGF. Controlled growth factor delivery with this system in an animal model of severe ischemia led to spatial control over vessel density, size, and maturity in the tissue within the scaffolds. In these studies, neovascular patterning was guided by the spatially segregated presentation of VEGF and PDGF. Similar to a previous study using focal applications of growth factor in multiple depots, vessel density increases were observed at 2 weeks, while effects on vessel maturity were observed out to 6 weeks (12). However, the resultant control over vascular patterning described in these studies resulted from angiogenesis alone at a site of *de novo* tissue formation and was achieved through spatio–temporal delivery of multiple growth factors with a single delivery vehicle. Application of this system may be extended to the combined delivery of other angiogenic growth factors (e.g. $VEGF_{121}$, Angiopoietin 1, Angiopoietin 2, TGF-β) that play important roles in this process (5, 15) or combinations of growth factors that act in different tissue regeneration processes (e.g. VEGF and BMPs) (26). The delivery system designed and investigated in these studies has potential utility in investigations of a variety of other growth factor-driven tissue regenerative processes, in addition to angiogenesis. For example, this system may be readily modified to mimic biologically relevant spatial and temporal complexities of signaling mechanisms in the regeneration of bone and cartilage, muscle, or nerve. The formation of more organized tissue structures through controlled delivery of growth factor combinations in physiologically relevant spatial profiles and sequences may also greatly enhance engineered tissue integration and functionality.

ACKNOWLEDGEMENTS

We gratefully acknowledge financial support from the NIH (R01 HL069957), and the Biological Resources Branch of the National Cancer Institute for providing VEGF for our studies.

REFERENCES

1. L. Coultas, K. Chawengsaksophak, and J. Rossant. Endothelial cells and VEGF in vascular development. *Nature* **438**:937–945 (2005).
2. L. C. Gerstenfeld, D. M. Cullinane, G. L. Barnes, D. T. Graves, and T. A. Einhorn. Fracture healing as a post-natal developmental process: molecular, spatial, and temporal aspects of its regulation. *J. Cell. Biochem.* **88**:873–884 (2003).
3. A. Eichmann, F. Le Noble, M. Autiero, and P. Carmeliet. Guidance of vascular and neural network formation. *Curr. Opin. Neurobiol.* **15**:108–115 (2005).
4. G. D. Yancopoulos, S. Davis, N. W. Gale, J. S. Rudge, S. J. Wiegand, and J. Holash. Vascular-specific growth factors and blood vessel formation. *Nature* **407**:242–248 (2000).
5. E. M. Conway, D. Collen, and P. Carmeliet. Molecular mechanisms of blood vessel growth. *Cardiovasc. Res.* **49**: 507–521 (2001).
6. C. Ruhrberg. Growing and shaping the vascular tree: multiple roles for VEGF. *BioEssays* **25**:1052–1060 (2003).
7. Y. Dor, V. Djonov, and E. Keshet. Making vascular networks in the adult: branching morphogenesis without a roadmap. *Trends Cell Biol.* **13**:131–136 (2003).
8. T. Boontheekul and D. J. Mooney. Protein-based signaling systems in tissue engineering. *Curr. Opin. Biotechnol.* **14**: 559–565 (2003).
9. R. R. Chen and D. J. Mooney. Polymeric growth factor delivery strategies for tissue engineering. *Pharm. Res.* **20**:1103–1112 (2003).
10. P. G. Campbell, E. D. Miller, G. W. Fisher, L. M. Walker, and L. E. Weiss. Egineered spatial patterns of FGF-2 immobilized on fibrin direct cell organization. *Biomaterials* **26**:6762–6770 (2005).
11. L. N. Luong, S. I. Hong, R. J. Patel, M. E. Outslay, and D. H. Kohn. Spatial control of protein within biomimetically nucleated mineral. *Biomaterials* **27**:1175–1186 (2006).
12. S. M. Peirce, R. J. Price, and T. C. Skalak. Spatial and temporal control of angiogenesis and arterialization using focal applications of VEGF164 and Ang-1. *Am. J. Physiol. Heart Circ. Physiol.* **286**:H918–925 (2004).
13. M. C. Peters, P. J. Polverini, and D. J. Mooney. Engineering vascular networks in porous polymer matrices. *J. Biomed. Mater. Res.* **60**:668–678 (2002).
14. Q. Sun, R. R. Chen, Y. Shen, D. J. Mooney, S. Rajagopalan, and P. M. Grossman. Sustained vascular endothelial growth factor delivery enhances angiogenesis and perfusion in ischemic hind limb. *Pharm. Res.* **22**:1110–1116 (2005).
15. T. P. Richardson, M. C. Peters, A. B. Ennett, and D. J. Mooney. Polymeric system for dual growth factor delivery. *Nat. Biotechnol.* **19**:1029–1034 (2001).
16. S. Cohen, T. Yoshioka, M. Lucarelli, L. H. Hwang, and R. Langer. Controlled delivery systems for proteins based on poly(lactic/glycolic acid) microspheres. *Pharm. Res.* **8**:713–720 (1991).
17. L. D. Harris, B. S. Kim, and D. J. Mooney. Open pore biodegradable matrices formed with gas foaming. *J. Biomed. Mater. Res.* **42**:396–402 (1998).
18. W. M. Saltzman. *Drug Delivery: Engineering Principles for Drug Therapy*. (eds.). Oxford University Press, London, UK, 2001.
19. R. B. Bird. *Transport Phenomena.* (eds.). Wiley, New York, 2001.
20. R. Bird, W. Stewart, and E. Lightfoot. *Transport Phenomena.* (eds.). Wiley, New York, 2002.
21. M. C. Peters, B. C. Isenberg, J. A. Rowley, and D. J. Mooney. Release from alginate enhances the biological activity of vascular endothelial growth factor. *J. Biomater. Sci. Polym. Ed.* **9**:1267–1278 (1998).
22. R. R. Chen, and D. J. Mooney. Host immune competence and local ischemia affects the functionality of engineered vasculature. *Microcirculation* **14**(2) (2007)
23. E. Stabile, M. S. Burnett, C. Watkins, T. Kinnaird, A. Bachis, A. la Sala, J. M. Miller, M. Shou, S. E. Epstein, and S. Fuchs. Impaired arteriogenic response to acute hindlimb ischemia in CD4-knockout mice. *Circulation* **108**:205–210 (2003).
24. T. Couffinhal, M. Silver, L. P. Zheng, M. Kearney, B. Witzenbichler, and J. M. Isner. Mouse model of angiogenesis. *Am. J. Pathol.* **152**:1667–1679 (1998).
25. K. K. Hirschi, S. A. Rohovsky, L. H. Beck, S. R. Smith, and P. A. D'Amore. Endothelial cells modulate the proliferation of mural cell precursors via platelet-derived growth factor-BB and heterotypic cell contact. *Circ. Res.* **84**:298–305 (1999).
26. Y. C. Huang, D. Kaigler, K. G. Rice, P. H. Krebsbach, and D. J. Mooney. Combined angiogenic and osteogenic factor delivery enhances bone marrow stromal cell-driven bone regeneration. *J. Bone Miner. Res.* **20**:848–857 (2005).